

The Jamming Transition in Granular Materials

Derek Vigil

Physics Department, University of Illinois Urbana-Champaign, Urbana, IL 61801

Abstract

We review the jamming transition in granular materials, especially as studied via simulation by Makse and O'Hern, and via experiment by Majmudar. In all three cases scaling behavior for pressure p and mean contact excess $Z - Z_c$ with $(\phi - \phi_c)$, where ϕ_c is the critical volume fraction, is found. Makse finds a dependence of ϕ_c on the rate of approach to criticality, i.e. compression (decompression) rate γ . O'Hern finds a dependence of the pressure critical exponent α on the type of potential, but not on dimensionality, while all three cases find the mean contact excess exponent β to be independent of both potential and dimension. Agreement is found between the experiments by Majmudar on granular systems composed of discs and the results of O'Hern for frictionless particles in a harmonic potential, indicating that the jamming transition is relatively insensitive to frictional effects. A comparison of the characteristics of the jamming transition and continuous phase transitions is made.

1 Introduction

Granular materials are ubiquitous in both nature and industry. Desire for optimization of processes in the latter, along with increasing attention to the physically interesting (and general) phenomenon of jamming, has led to an increased level of research into granular materials. The jamming transition is of interest because of the possibility of wide applicability of the concept in granular systems, colloidal systems, glasses, and emulsions [1].

The jamming transition as a general phenomenon is a critical slowing down of the dynamics of a system far from equilibrium due to "overcrowding" of particles. This overcrowding can be effected either by a compression of the particles, or in the case of attractive liquids, by lowering the temperature [2, 3]. With few paths open for particle movement, the dynamics of the system are arrested [4, 5]. It is this arrest of the dynamics to which jamming refers. In the case of attractive liquids this phenomenon is better-known as the glass transition, which has been widely studied, but is still poorly understood.

The phenomenon of jamming has a much different nature in liquid systems and granular systems. Liquid systems, composed of atoms, are thermal, while macroscopic granular systems have a large gravitational energy that makes them insensitive to thermal effects, or athermal [6]. Thermal fluctuations are not large enough to move granular particles and,

hence are unable to unjam a jammed granular system as they are able to unjam a glass system at high enough temperatures. However, a shear stress can effect such an unjamming, so that an effective temperature defined in terms of the shear stress is a variable in granular systems that can play a role analogous to temperature in liquid systems [7, 8]. Such considerations have led to a proposal of a jamming phase diagram by Liu and Nagel [1]. This phase diagram is shown in Figure 1. The $1/\phi - T$ plane, where ϕ is the volume fraction of particles, corresponds to the situation for fluids, while the $1/\phi - \Sigma$ plane, where Σ is the shear stress, corresponds to the situation for granular systems. Systems that fall beneath the jamming surface, i.e. those at high volume fraction and low temperature, shear stress, will be jammed, while systems lying above the jamming surface will not be jammed.

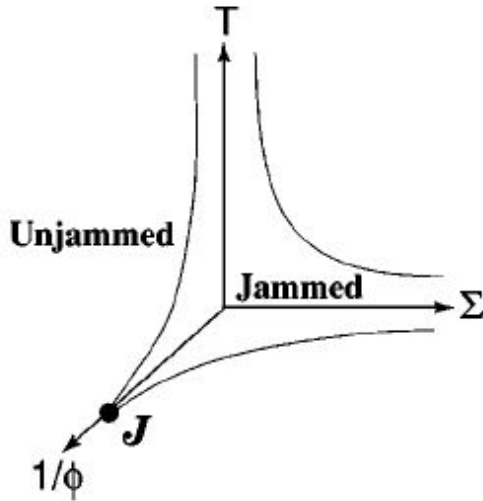


Figure 1: Jamming phase diagram, as first proposed by Nagel and Liu[1] and adapted by O’Hern et. al.[9]. The point **J** corresponds to temperature T and shear stress Σ both equal to zero.

In this paper we review 3 studies of the jamming transition in granular systems, 2 computational and 1 experimental [4, 9, 10, 11]. All three studies involve compressing or decompressing a sample of granular particles until there is a transition to or from a packing with nonzero pressure, respectively. The value of the volume fraction at which this transition occurs is the critical volume fraction ϕ_c for jamming. Nonzero pressure is taken as the condition for jamming because for nonjammed configurations the particles can shift around until a configuration is reached in which there is zero net pressure in the system. Makse et. al. employ a time-stepped MD solution to Newton’s force and torque equations for a Hertz-Mindlin force law to study the jamming transition [4], while O’Hern et. al. use an energy minimization technique [9, 10], and Majmudar et. al. run experiments on photoelastic discs in a size-adjustable box [11]. It is found in all cases that the jamming transition resembles

other continuous transitions in that it exhibits power-law behavior in pressure p and excess contact number $Z - Z_c$ above the critical volume fraction ϕ_c . However, the jamming transition also exhibits some properties very different from those of continuous phase transitions, including a dependence of the critical volume fraction ϕ_c on the rate of compression or decompression (i.e. the rate of approach to the critical point) found in the Makse simulations, a dependence of the pressure critical exponent on potential, but not dimensionality and a lack of fluctuations in all physical quantities of interest on approach to ϕ_c from below found in the O'Hern simulations, and a discontinuity in the mean contact number Z upon moving from above to below ϕ_c found in both simulations and the Majmudar experiment. After reviewing the methods and data of these simulations and experiments we will discuss the implications of their findings.

2 Methods

The two simulation papers considered employ different methods in their studies of jamming in granular materials. Makse and Zhang [4] use a time-stepping, finite-difference method for solving Newton's force and torque equations for every particle in the 3-dimensional system. The interaction between two spherical particles of radii R_1 and R_2 at positions \vec{x}_1 and \vec{x}_2 is modeled by a nonlinear Hertz-Mindlin interaction, where the tangential and normal forces are given by:

$$F_n = \frac{2}{3}k_n R^{1/2} \xi^{3/2} \quad (1)$$

$$F_t = \int_{path} k_t (R\xi)^{1/2} ds \quad (2)$$

In (1) and (2) R is the geometric mean of R_1 and R_2 , $R = 2R_1R_2/(R_1 + R_2)$ and ξ is the normal overlap of the two particles, $\xi = (1/2)(R_1 + R_2 - |\vec{x}_1 - \vec{x}_2|)$. Also, $k_n = 4G/(1 - \nu)$ and $k_t = 8G/(2 - \nu)$, where G is the bulk modulus and ν is the Poisson ratio of the material from which the granules are constructed. The normal force is only valid for compression, so that $F_n = 0$ for $\xi < 0$. The path that the integral in (2) is taken around is that from the initial condition $F_n = F_t = 0$ at $\xi = s = 0$, where s is the tangential displacement. In the limit of large tangential displacement s , the expression for the tangential force simplif

$$F_t = \mu F_n \quad (3)$$

where μ is a friction coefficient.

The system is composed of 10^4 glass particles of radius 0.1 mm in a periodically repeating cubic box. The protocol for studying the jamming behavior is to start the system in a state with the particles randomly placed and non-overlapping in a box at volume fraction $\phi \approx 0.2$. Then the box is compressed isotropically at a rate γ until a desired volume fraction ϕ is reached. The system is then allowed to relax at constant volume until a stable state is reached, where by a stable state it is meant that the pressure remains constant over some time relatively long interval. The value of the volume fraction ϕ_c below which the system cannot sustain a nonzero pressure, and above which the pressure scales as $(\phi - \phi_c)^\alpha$ is called the critical volume fraction.

O'Hern, et. al. [9, 10] take a much different approach, generating five different random configurations of particles for a given value of the volume fraction ϕ and then minimizing the potential energy of the resultant configurations using conjugate-gradient techniques. If the energy-minimizing state has zero pressure, then the system is compressed by increasing the radii of the all particles by the same fraction, with another round of conjugate-gradient minimizing following each compression. When the compressed, energy-minimizing state has a nonzero pressure then the critical volume fraction ϕ_c has been reached. Conversely, if the energy minimizing state has nonzero pressure, then the system is decompressed by decreasing the radii of all of the particles by the same fraction, with further rounds of conjugate-gradient minimizing following each decompression, until the pressure goes to zero at the critical volume fraction ϕ_c . This procedure was carried out for various potentials in both 2 and 3 dimensions. The potentials between two particles i and j whose centers are separated by a distance $r_{ij} = |\vec{x}_i - \vec{x}_j|$ used by O'Hern et. al. are of the form

$$V(r_{ij}) = \epsilon (1 - r_{ij}/\sigma_{ij})^\theta / \theta \quad (4)$$

for $r_{ij} < \sigma_{ij}$ and zero otherwise, where ϵ is the energy scale of the interaction, σ_{ij} is the sum of the radii of the particles i and j , $\sigma_{ij} = R_i + R_j$. The value of ϵ is taken to be positive and the different values of θ for which the jamming transition are investigated are $3/2$, 2 , and $5/2$, corresponding to repulsive nonlinear, repulsive linear, and repulsive hertzian springs. Note that the use of potentials of this form implies that these simulations were carried out for frictionless particles, in contrast to the frictional systems considered by Makse and by any experiment. The system size in 2D (3D) is 1024 (512) particles, except for in the simulations where the investigators are examining finite-size effects, in which case the number of particles is allowed to vary between 4 and 4096. A 50:50 mixture of spheres with size ratio 1.4 are used in the 2D simulations in order to prevent crystallization, while both this bidisperse configuration and a monodisperse configuration are studied for the 3D simulations.

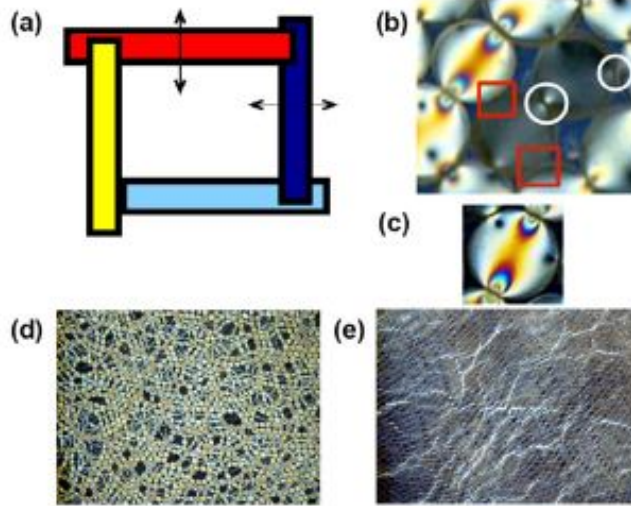


Figure 2: Experimental setup for the Majmudar et. al. paper. (a) The photoelastic discs are placed in the adjustable size cell. The cell area is then either reduced or increased, depending on the initial state of the discs. The cell is horizontal and a camera lies above the setup to capture the data. Crossed circular polarizers are used to obtain the stress data.(b) and (c) show discs under stress, while (d) and (e) show a highly compressed/jammed and nearly unjammed state, respectively.

Majmudar et. al. [11] use a system of birefringent discs to observe the jamming transition. Specifically, an 80:20 mixture of 3000 small and large photoelastic, or birefringent under stress, discs are placed in a 42 cm by 42 cm horizontal cell with two movable walls. The smaller discs of diameter 0.74 cm are more numerous than the larger discs of diameter 0.86 cm. The setup is shown in Figure 2.

The walls can move in increments of $40\mu\text{m}$, which is approximately $0.005D$, where D is the diameter of the discs. Behavior near the jamming transition is studied in a similar way as is done in the Makse simulations: for systems with zero pressure initially, i.e. zero stress, the box is compressed until a nonzero pressure is obtained, while for systems with nonzero pressure initially the box is decompressed until a zero pressure is obtained. In this way the critical volume fraction ϕ_c and the power-law behavior for pressure p and mean contact number Z as a function of $(\phi - \phi_c)$ are observed. The pressure p is calculated from the stress data, which is collected using crossed circular polarizers and a CCD camera that lies above the cell. The mean contact number is recorded from direct visual observation. Note that, again, the purpose of having a mixture of disc sizes is to prevent crystallization.

3 Results

Makse et. al. study the dependence of the mean contact number Z and the pressure p on $(\phi - \phi_c)$ for 4 different compression rates γ , 2×10^y m/s, $y = 1, 2, 3, 4$. The purpose of studying the transition for 4 different compression rates is to determine the effect of the rate of approach to criticality for the jamming transition. The lowest compression rate, for $y = 1$, corresponds to a compression of 1×10^{-7} of a particle diameter per MD step. The results are shown in Figure 3.

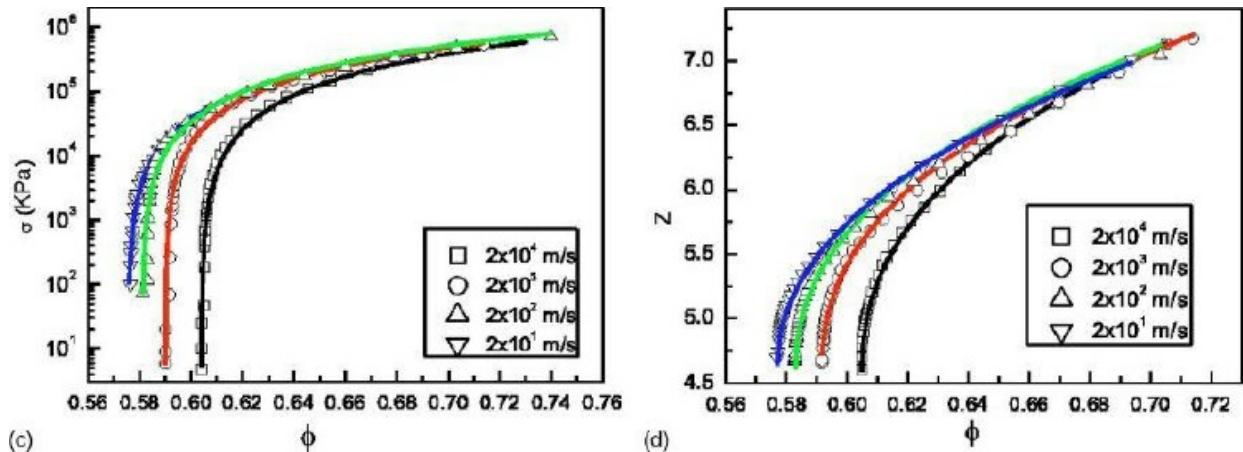


Figure 3: Pressure p (c) and mean contact number Z (d) as a function of volume fraction ϕ for different compression rates γ from the Makse simulations. There is a power-law growth in the pressure p and in the mean contact excess $Z - Z_c$ above the critical volume fraction ϕ_c . Note that critical volume fraction, at which the power-law growth begins, is different for each compression rate γ , indicating a dependence of the jamming on this dynamical parameter.

Power law behavior is observed in both the pressure p and mean contact excess $Z - Z_c$, i.e through fitting the simulation data it is found that

$$p \sim (\phi - \phi_c)^\alpha \quad (5)$$

$$Z - Z_c \sim (\phi - \phi_c)^\beta \quad (6)$$

The values for Z_c , ϕ_c , α , and β for the different compression rates are given in Table I. An interesting feature of the transition is that the value of the critical volume fraction ϕ_c depends on the compression rate γ . This dependence of the critical point on the rate of approach to the critical point is not typical of continuous phase transitions. The values of the exponents α and β are roughly 0.46 and 1.50 for all of the different compression rates, while Z_c is found to be approximately 4.53, regardless of compression rate .

Table 1: Values of the critical mean contact number and volume fraction, and the critical exponents α and β obtained from fitting the data from the Makse simulations for different values of the compression rate γ .

γ (m/s)	ϕ_c	Z_c	α	β
2×10^4	0.604	4.52	1.52	0.46
2×10^3	0.590	4.53	1.46	0.45
2×10^2	0.581	4.53	1.48	0.46
2×10^1	0.576	4.54	1.52	0.47

O’Hern et. al. study the dependence of the mean contact excess $Z - Z_c$ and the pressure p on $(\phi - \phi_c)$ for a constant compression rate, but for differing values of the polydispersity, the parameter θ in (4), and the dimensionality D . They find that the exponent $\beta \approx 0.48$ regardless of polydispersity, potential, and dimensionality, while the exponent α is dependent on potential and its relation to the parameter θ is given approximately by

$$\alpha = \theta - 1 \tag{7}$$

The critical mean contact number Z_c is dimension dependent, $Z_c \approx 2D$. The data for one of the given starting configurations for each combination of the polydispersity, θ , and D are given in Figure 4 (for pressure only) and Table 2. The data for $\theta = 3/2$ is omitted because all trends can be seen from considering just the cases $\theta = 5/2, 2$. Note that both the pressure and the mean contact excess above ϕ_c were fit as a function of $(\phi - \phi_c)$. Indeed, the authors remark that ϕ_c differs for each initial configuration that they generate, but the behavior of p and $Z - Z_c$ as a function of $(\phi - \phi_c)$ is identical for each initial configuration. It would seem that, in not concerning themselves with the variation of ϕ_c with changing initial configurations, the authors see this as an artifact of the simulation procedure that is to be neglected. The validity of such a view cannot be judged by me, as it is far beyond my level of expertise. Nonetheless, it should be noted because it is in direct contrast to the situation in the Makse paper, where the variation of ϕ_c is part of what is being studied.

The fact that the exponent α depends on the nature of the potential and not the dimensionality of the system is counter to the usual situation with continuous phase transitions, in which dimensionality often comes into the critical exponents, but the exponents are unperturbed by changes in potential. The result that β is independent of dimension and potential seems reminiscent of mean-field theory. The mean critical contact number is determined by the isostatic condition, in which the total number of contacts is directly proportional to the number of force equations that must be solved, which clearly varies with dimension. Hence the dependence of Z_c on dimension. Note that the values of α and β for the hertzian $\theta = 5/2$ potential in 3 dimensions match those obtained in the Makse simulations, as would

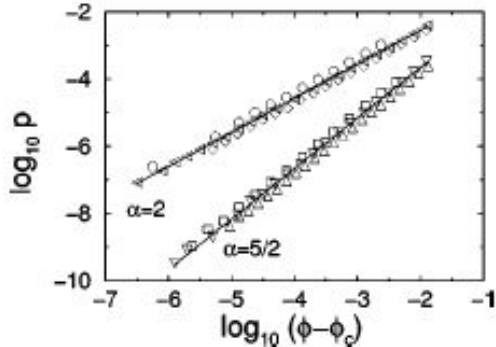


Figure 4: $\log(p)$ versus $\log(\phi - \phi_c)$ for the O’Hern simulations. The power-law behavior is apparent. The lines labeled $\alpha = 2$ and $\alpha = 5/2$ correspond to the data for the simulations in which the potentials have $\theta = 2$ and $\theta = 5/2$, respectively. The notation in the O’Hern paper has been changed to match that in the Makse paper. Both the $\theta = 2$ line and the $\theta = 5/2$ line contain data for the simulations with 3D monodisperse, 3D bidisperse, and 2D bidisperse particles. All data has collapsed onto lines of slope $\alpha = 1$ and $\alpha = 3/2$ respectively, as given by equation (7).

be expected given the force law and dimensionality used in the Makse simulations. The fact that Z_c is different in the two simulations is due to the sensitivity of Z_c to frictional effects [4], since friction is the aspect in which the condition of the systems in these two simulations differ.

Table 2: Values of the critical mean contact number and volume fraction, and the critical exponents α and β obtained from fitting the data from the O’Hern simulations for different values of dimension D , potential parameter θ , and polydispersity.

D	Polydispersity	θ	α	β	Z_c
2	Bi	2	1.01	0.49	3.98
2	Bi	5/2	1.50	0.48	3.98
3	Bi	2	1.03	0.47	5.98
3	Bi	5/2	1.51	0.49	5.98
3	Mono	2	1.01	0.51	5.98
3	Mono	5/2	1.50	0.47	5.98

In addition to the neglected variation in ϕ_c with different initial configurations, it is found that ϕ_c is dependent on dimensionality and system size, but not on the type of potential (e.g. not on θ) or polydispersity. The data showing this is given in Figure 5, which gives the probability distribution of ϕ_c for the various conditions under study. We see from figure from Figure 5 that the effect of increasing system size is to increase the value of ϕ_c at which $P(\phi_c)$ peaks up to some asymptotic value, which is found by fitting to be $\phi^* = 0.639 \pm 0.001$ for the 3 dimensional system. Increased system size also gives a more sharply peaked distribution, so that for large systems the value of ϕ_c at which $P(\phi_c)$ peaks is effectively the value of ϕ_c for all configurations. The value of this asymptotic value is not given in the 2-dimensional

case, but from Figure 5(b) appears to be approximately 0.84. This dependence of the critical point on the dimensionality and on the system size for the jamming transition is similar to the situation for continuous phase transitions.

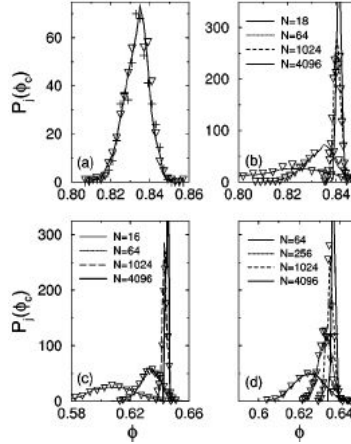


Figure 5: The probability distribution for the critical volume fraction $P(\phi_c)$ for various conditions. In (a)-(d) the line is not a fitting line, but gives the probability distribution for $\theta = 2$. The probability distributions for $\theta = 3/2$ and $\theta = 5/2$ are given by pluses and downward triangles, respectively. (a) gives $P(\phi_c)$ for $\alpha = 3/2, 2, 5/2$ for a system of $N = 64$ particles. It is clear that the data for the different potentials collapses onto one curve. (b), (c), and (d) give $P(\phi_c)$ for $\alpha = 2, 5/2$ for various system sizes. (b) gives $P(\phi_c)$ for a 2D bidisperse system, while (c) gives $P(\phi_c)$ for a 3D bidisperse system and (d) gives $P(\phi_c)$ for a 3D monodisperse system. Comparison of (c) and (d) shows that the polydispersity has no effect on the distribution, while comparison of (b) with (c) and (d) shows that dimensionality does have an effect on the distribution, shifting the large system ($N=4096$) peak to 0.84 in the 3D systems of (c) and (d) from the value 0.64 for the 2D system of (b). The peaks of the distribution $P(\phi_c)$ for all other system sizes are similarly shifted.

Majmudar et. al. find in their experiments with the compression of photoelastic discs that the critical volume fraction is $\phi_c = 0.8422$, while the critical exponents have values $\alpha \approx 1.1$, $\beta \approx 0.55$. The exponents are extracted by excluding rattlers, which are discs having less than 2 contacts and which are found to decrease exponentially as a function of $(\phi - \phi_c)$ above ϕ_c , hence justifying their neglect in calculating the exponents. ϕ_c is found by locating the value of ϕ where Z starts to rapidly, almost discontinuously, increase. The experimentally obtained values of the critical exponents and the critical volume fraction ϕ_c are close to the values found by O'Hern et. al. for frictionless particles in harmonic potentials, regardless of polydispersity and dimension. This indicates, the authors conclude, that friction has a small affect on the jamming transition in granular materials. The data for this experiment is shown in Figure 6.

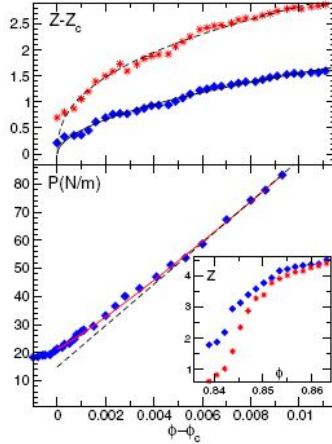


Figure 6: Data for the Majmudar experiments. In the top panel the stars (squares) are for the case with (without) rattlers, while in the bottom panel the solid (dotted) line is for the case with (without) rattlers. The $\beta \approx 0.55$ and $\alpha \approx 1.1$ power-law dependence of mean contact excess $Z - Z_c$ and pressure p , respectively, on $(\phi - \phi_c)$ can be seen.

4 Discussion and Conclusions

A first comment that must be made before interpreting the presented results is that the field of granular materials, especially the theoretical description of granular materials, is a new and diverse, and therefore poorly understood, field. Indeed, the confused state of affairs has led Aranson and Tsimring to comment that "the theoretical description of granular systems remains largely a plethora of different, often contradictory concepts and approaches" [6]. Hence, there is still much ambiguity in interpreting experimental and computational results, since there is no set theory by which to judge them.

Probably the most easily discussed result is the fact that the critical exponents for the Majmudar experiments best agree with the system of frictionless particles in a harmonic potential studied by O'Hern. This is perhaps surprising since one might think that real discs would show the effects of friction more prominently. However, in a previous experiment Majmudar and Behringer have found that frictional forces are only a tenth of the normal forces in a physical granular system [12], so that it is understandable that frictional effects do not have a large effect on the jamming transition given their small magnitude relative to the normal forces present in the system.

With the caveat give above in mind we examine the results of the simulations and experiments, as there is much in the data that is of interest, especially in relation to continuous phase transitions. First of all, the power-law behavior in p and $Z - Z_c$ above the critical volume fraction ϕ_c is similar to the situation for continuous phase transition, e.g. the Ising ferromagnet. Additionally, in data not presented here, but covered in the 2003 paper by

O'Hern et. al. [9] it was found that the width and peak of the distribution $P(\phi_c)$ scale with system size. This finite-size scaling is also consistent with what is observed in continuous phase transitions. However, there are many other aspects of the jamming transition in granular systems that make it very different from continuous phase transitions. The shift in the critical volume fraction ϕ_c with variation of the compression (or decompression) rate, i.e. the rate of approach to criticality, is unlike what is seen in continuous phase transitions, as is the lack of fluctuations in quantities such as energy, pressure, etc. as the ϕ_c is approached from below, as found in the O'Hern simulations [9]. Also, the dependence of the pressure critical exponent α on the type of potential, but not on dimension is inconsistent with what would be expected from continuous phase transition theory and considerations of upper critical dimension and universality classes, as discussed by O'Hern [9]. Finally, in yet another result from O'Hern, it was found that there was rounding of the power-law behavior for smaller system size for systems at constant volume, but not for systems at constant pressure. This difference between the constant volume and constant pressure cases, and the lack of finite-size effects for constant pressure systems, is not typical of ordinary critical phenomena O'Hern makes clear, though I am unable to verify this claim [9].

Thus, it would appear that the jamming transition cannot be easily placed into the usual continuous phase transition framework without some sort of substantial modification. Not possessing the requisite theoretical granular material background, I am unable to suggest any sort of modification. However, it is clear from the Makse simulations that the RG framework would need some modification to account for the variability of the critical point with varying rates of approach to criticality. This dynamical aspect of the jamming transition does not fit into the usual RG framework, in which fixed points are determined by equations involving coupling constants in the Hamiltonian, which are taken to be static. This is perhaps to be expected since RG is for systems in equilibrium, whereas the jamming transition in granular materials involves a system far from equilibrium. Perhaps some sort of adaptation of the framework can be found which would allow calculation of the various properties of the jamming transition in granular materials. At the present the development of such an adaption seems daunting, but with many of the best minds in physics trained to an area of research that could perhaps lead to the reinvention of "statistical mechanics in a new context" [13] maybe it is not too far-fetched to think that just this adaptation is in the works.

References

- [1] A.J. Liu and S.R. Nagel. *Nature*, 396:21, 1998.
- [2] C.A. Angell M.D. Ediger and S.R. Nagel. *J. Phys. Chem*, 100(13):200, 1996.
- [3] P.G. Debenedetti and F.H. Stillinger. *Nature*, 410:259, 2001.
- [4] H.P. Zhang and H.A. Makse. *Phys. Rev. E*, 72:011301, 2005.
- [5] H. J. Herrmann A. Coniglio, A. Fierro and M. Nicodemi, editors. *Unifying Concepts in Granular Media and Glasses*. Elsevier, Amsterdam, 2004.
- [6] I.S. Aranson and L.S. Tsimring. *Rev. Mod. Phys.*, 78:641, 2006.
- [7] J. Kurchan L.F. Cugliandolo and L. Peliti. *Phys. Rev. E*, 55:3898, 1997.
- [8] L. Berthier and J.L. Barrat. *PRL*, 89:095702, 2002.
- [9] A.J. Liu C.S. O'Hern, L.E. Silbert and S.R. Nagel. *Phys. Rev. E*, 68:011306, 2003.
- [10] A.J. Liu C.S. O'Hern, S.A. Langer and S.R. Nagel. *PRL*, 88:075507, 2002.
- [11] S. Luding T.S. Majmudar, M. Sperl and R.P. Behringer. *PRL*, 98:058001, 2007.
- [12] T.S. Majmudar and R.P. Behringer. *Nature*, 435:1079, 2005.
- [13] L.P. Kadanoff. *Rev. Mod. Phys.*, 71:435, 1999.